Influence of Apparent Contact Pressures and Groove Parameters in Contact Simulation with Tribological Surface Textures

Muhammad Taureza[1,], Sylvie Castagne[1], Samuel Lim Chao Voon[2]*

[1]School of Mechanical and Aerospace Engineering, Nanyang Technological University, Singapore, Singapore

[2]Forming Technology Group, Singapore Institute of Manufacturing Technology, Singapore, Singapore

** Corresponding author's e-mail address: m090051@e.ntu.edu.sg*

Abstract – The influence of groove parameters to friction at different apparent contact pressures was investigated through finite element simulations using three different fundamental friction laws in order to understand the friction-reducing mechanism of tribologically textured-surface in experiments. The behavior was presented as combined effects of reducing friction by reducing load bearing area and increasing friction from plowing by the surface textures. A case was also presented to illustrate how multi scale modeling can be used to design a metal forming process involving textured tooling.

Keywords – friction models, tribological surface textures, finite element method, multiscale modeling

I. INTRODUCTION

The miniaturization of metal forming tooling and workpiece to sub-millimeter sizes (or microforming size [1]) has shown a trend of increasing friction [1, 2] which can be explained using the lubricant pocket model [2]. Increased friction in metal forming systems generally results in undesirable increase in process load requirement, tool wear and workpiece damage.

Outside the context of metal forming processes, studies on tribological surface texturing on metallic surfaces have been shown to reduce friction both in lubricated [3] and unlubricated condition [4] and the implementation of tribological surface texturing to reduce friction in sheet metal forming friction test has been exemplified using strip drawing test [5]. However, studies on tribological surface texturing focus mostly on experiments with no strong theory to explain the friction-reducing behavior.

This paper briefly summarizes results from past studies involving tribological surface textures and presents a finite element approach to simulate contact when surface textures are present. The contact pressure dependent behavior and the influence of groove parameters were further investigated and ultimately, implementation of multi scale simulation and conclusions based on simulation results are presented.

II. SURFACE TEXTURES

Tribological surface textures are highly defined surface features deliberately introduced with the objective of friction control. Methods such as laser surface texturing (LST), lithography, abrasive jet machining and embossing using hard tool have been explored as means of producing surface textures.

Results on surface texturing have been published with mainly two geometries –parallel grooves and pores/dimples and findings suggested that there are optimum texture parameters (distribution/area density [6], size [7], geometry [8]) to produce the lowest friction.

For unlubricated contact, the friction reducing behavior of surface textures was explained by entrapment of wear particles [9]. However, the friction-reducing behavior started to take effect early in the experiment [4, 9]. According to the delamination theory of wear [10], the wear sheets are generated following continuous sliding of surfaces which gradually creates sub-surface micro-cracks. The coalescing micro-cracks then results in removal of wear sheets or particles. Therefore, the friction-reducing behavior noticed at the beginning of the experiment cannot be attributed to entrapment of wear particles as the particles may not have been generated.

On the other hand, in lubricated contact, the friction-reducing performance of surface textures was explained by the mechanism of trapping liquid lubricant in the surface textures enabling lubricant to stay at the interface longer in the case of boundary lubrication [6] and enhancing hydrodynamic lubrication [11] in the case of full film lubrication.

Reference [3], however, showed that even when the lubricant was always present at the contact (experimental setup immersed in lubricant), the textured surface still produced lower friction in comparison to the untextured surface. These findings suggest that while surface texturing was proven to reduce friction by means of wear particles and lubricant entrapment, there is another explanation for the friction reduction beyond the context of wear particle and lubricant entrapment, i.e. the definitions of friction behavior themselves.

III. FRICTION MODELS

Different friction models were used in the contact simulation to assess the influence of texture geometry on friction:

1) Coulomb Friction Model [12, 13]

$$\tau = \mu p, \tag{1}$$

with τ representing the friction stress, μ the Coulomb friction coefficient and p the normal pressure. Reference [12] proposed that magnitude of friction is proportional to the true contact area –a small percentage of the apparent contact area. Mating surfaces come into contact at their asperities forming the true contact area. With increasing *apparent* normal pressure, true contact area and friction increase.

2) Constant Friction Model [13, 14]

$$\tau = mk, \tag{2}$$

with m the friction factor and k the shear flow stress. Coulomb model dictates that friction increases with normal

pressure and true contact area. Constant friction model was first proposed to provide a solution at higher normal pressure when the true contact area approaches the apparent contact area. This threshold of low and high normal pressure is usually associated with the material's yield strength.

3) General Friction Model [14, 15]

$$\tau = f\alpha k, \quad (3)$$

with f and α representing the friction factor and ratio of real to apparent contact area. Equation (3) can be rewritten using dimensionless proportionality equations to relate contact pressure to real area of contact using material dependent proportionality limits (p^*, τ^*) [16, 17]:

$$\left(\frac{\tau}{k}\right) = \left(\frac{\tau^*}{k}\right)\frac{\left(\frac{p}{\sigma_0}\right)}{\left(\frac{p^*}{\sigma_0}\right)} \quad \text{for } \left(\frac{p}{\sigma_0}\right) \le \left(\frac{p^*}{\sigma_0}\right) \quad (4)$$

and

$$\left(\frac{\tau}{k}\right) = \left(\frac{\tau^*}{k}\right) + \left(f - \left(\frac{\tau^*}{k}\right)\right)\left(1 - \exp\frac{\left(\left(\frac{p^*}{\sigma_0}\right) - \left(\frac{p}{\sigma_0}\right)\right)\left(\frac{\tau^*}{k}\right)}{\left(f - \left(\frac{\tau^*}{k}\right)\right)\left(\frac{p^*}{\sigma_0}\right)}\right) \quad (5)$$

otherwise. σ_0 represents the flow stress and the proportionality limits are defined considering the development of slip line fields using zero angle asperity (flat surface) [16, 17]:

$$\left(\frac{\tau^*}{k}\right) = 1 - \sqrt{1 - f} \quad (6)$$

and

$$\left(\frac{p^*}{\sigma_0}\right) = \frac{1 + \left(\pi/2\right) + \arccos f + \sqrt{1 - f^2}}{\sqrt{3}\left(1 + \sqrt{1 - f}\right)} \quad (7)$$

The general friction model was proposed to obtain more accurate description of friction since Coulomb friction model overestimates friction at high normal pressure and constant friction model overestimates friction at low normal pressure and was originally presented specifically for metal forming applications. Even though this model was reported to be inaccurate when strain hardening is experienced in experiment [18], this model is generally accepted as more accurate than former models.

IV. SIMULATION SETUP

In order to have great details in interaction definition as well as computational efficiency simultaneously, this paper employs multi scale (meso-macro) contact simulation as presented in Table 1.

Commercial finite element code Abaqus/Standard with plane strain geometry was used for the mesoscale simulations. The simulation setup assumed textured tooling (parallel grooves aligned perpendicular to sliding direction) with elastic material model and flat-surfaced workpiece (Fig. 1) which used structured mesh based on asperity plowing simulation setup in [19] with elastic-plastic material definition to simulate copper workpiece.

The workpiece was fixed in space with periodic boundary condition to simulate periodicity of contact between the textured tooling and workpiece, sliding and indentation movement was introduced simultaneously on the tooling whilst reaction forces were recorded from the bottom nodes of the workpiece.

The simulation parameters and dimensions (i.e. period, heights, length, and radius) in relative size as well as elastic-plastic material definition based on Young's modulus (E) of 120 GPa, Poisson's ratio (v) of 0.33, yield strength of 300 MPa, as well as strain hardening definition using strength coefficient (K) of 317 MPa and work-hardening exponent (n) 0.51 representing annealed pure Copper [20] are presented in Table 2 and Fig. 2.

There are two different friction concepts in this study: *friction models* and *effective friction*. *Friction models* were used as friction definition in the simulation involving different texture geometry. The reaction forces recorded from the workpiece domain represent how the textures affect *effective friction*, i.e. flat surface will return the original friction model as effective friction.

This effective friction is then included in macroscale simulation using Deform 2D. The effective friction substitutes both the friction model and the textured surface to avoid the impracticality of simulating the full textured surface.

V. MESOSCALE SIMULATION RESULTS

Simulation involving elastic tooling (E 210 GPa, v 0.3) and elastic-plastic workpiece material definition (Fig. 2) was conducted to investigate the influence of friction models and groove geometry on the friction readout.

TABLE 1 Multi scale simulation

Simulation Scale	Input	Output
Meso (Abaqus/Standard)	Textured Surface + Friction Model	Effective Friction
Macro (Deform 2D)	Smooth Surface + Effective Friction + Process Geometry	Process Load Metal Flow

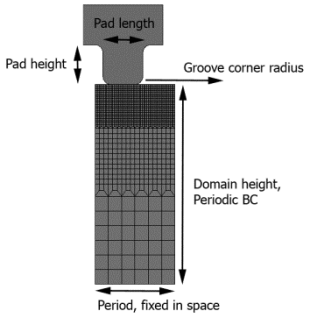

Fig. 1 Mesoscale simulation setup

TABLE 2 Mesoscale simulation parameters

Fixed geometry (relative size)		Variable geometry (relative size)	
Period	2	Groove radius	0.1 0.2 0.5
Domain height	5		
Pad length	1		
Pad height	1		
Material properties		**Friction laws**	
Tool (Elastic)	E = 210 GPa	Coulomb Friction Coefficient	0.2 0.5 1.0
WP (Elastic-Plastic)	See Fig. 2	Constant Friction Factor	0.2 0.5 1.0
		General Friction Factor	0.2 0.5 1.0

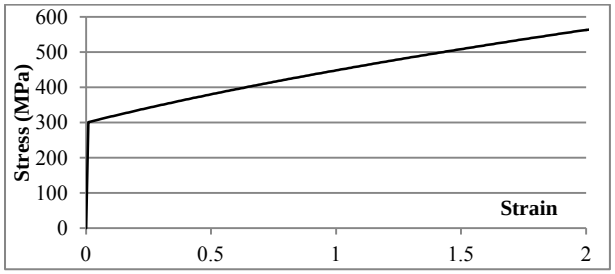

Fig. 2 Elastic-plastic material model

Effective friction coefficients (μ_{eff}) were acquired at different nominal contact pressure for different surface textures. Different friction models and corresponding coefficients/factors were then compared to examine how the surface textures fundamentally affect effective friction (τ_{eff}, Equation 8).

$$\tau_{eff} = \mu_{eff}\, p_{app} \quad (8)$$

The value of μ_{eff} was obtained from the ratio of total tangential reaction forces normalized to an absolute value and the total normal reaction forces (Equation 9, 10)

$$\tau_{eff} = \sum RF_1 \quad (9)$$

$$p_{app} = \sum RF_2 \quad (10)$$

with subscript 1 and 2 denotes sliding and normal direction, respectively. The notation p_{app} is used exclusively when surface textures are present. In a typical macroscale simulation, the surface asperities are represented by friction coefficient or factor. In this mesoscale simulation with surface textures, the asperities interaction is also represented by the friction definition. However, the engineered surface textures are simulated as are. In which case the notation p_{app} represents the average contact pressure read from the simulation to avoid having to distinguish the surface regions in and the regions not in contact.

In Coulomb friction model, τ is directly proportional to the p. Regardless of the surface texture geometries the effective friction returns the value of the Coulomb friction coefficient (Fig. 3) as the reduced load bearing area increases p at the textures.

The sudden increase of friction readout (marked by circles in Fig. 3) corresponds to the onset of workpiece plowing by the surface textures. Textures with larger corner radius (smaller load bearing area) start plowing the workpiece surface at lower nominal contact pressure (p_{app}) when elastic-plastic workpiece definition was used. Beyond the onset of plowing, the friction reading is no longer only attributed to the friction models, but also to macroscopic plowing by the textures (to distinguish from asperities plowing).

Nevertheless, this simulation does not reach nominal contact pressure above 500-600 MPa. The design of the surface texture allows the softer material to flow into the recess after increased displacement of the tooling (Fig. 4). This results in the indefinite increase of effective friction coefficient in all simulations. In order to simulate higher nominal contact pressure, the simulation must be allowed to plow deeper into the workpiece creating "pile-up" and hence subsequent sliding will have very high τ_{eff}.

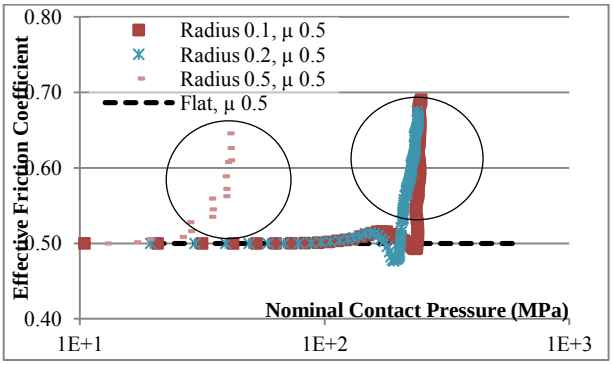

Fig. 3 Coulomb friction

When constant model was used (Fig. 5) at low nominal contact pressure, τ_{eff} was reduced as the load bearing area decreased. Hence, the groove with largest corner radius produced the lowest τ_{eff} at low nominal contact pressure. In constant friction model, the τ is constant regardless of the p. Therefore the overall friction is proportional to the load bearing area.

Similarly for general friction model, there is a concept of maximum friction stress when the p/σ exceeds the proportionality limit (Eq. 5 and Eq. 7). Therefore, at low p_{app}, simulation returned constant τ_{eff} and as the contact pressure exceeds the proportionality limit, effective friction coefficient was reduced (Fig. 6). Ultimately, this model shows the combination between Coulomb friction and constant friction.

It is also shown that there are competing behaviors between the friction-reducing effect from the smaller load bearing area (dominant at low nominal contact pressure) and the workpiece plowing effect (dominant at high p_{app}) as also observed in Coulomb friction model (Fig. 3). A *useful surface texture* should produce friction lower than the friction produced by flat surface with the same friction factor.

With constant friction model with m of 0.5 considered (Fig. 5), texture with radius 0.5 produces the lowest friction. However, this texture reaches onset of workpiece plowing earliest and thus the texture is only useful when p_{app} is lower than 200 MPa.

In contrast, the texture with radius 0.1 does not produce the lowest friction when p_{app} is below 120 MPa. Nevertheless this texture geometry is useful for wider range of p_{app} (up to 500 MPa) and crucially the contact pressure in metal forming system will exceed the yield strength of the workpiece (300 MPa in this case). At 300 MPa and m of 0.5, groove surface textures with radius 0.1 produces one-fourth the friction when flat surfaces are considered.

When general friction model is considered (Fig. 6), surface textures can lower friction marginally for the case of f = 0.5. Similar competing behaviors of friction reduction and workpiece plowing were shown. At 300 MPa, surface textures of both radius 0.1 and 0.2 produce 60% of the friction between flat surfaces, and the useful limits are up to 500 and 420 MPa p_{app}, respectively, while texture with radius 0.5 shows very narrow useful range (below 90 MPa).

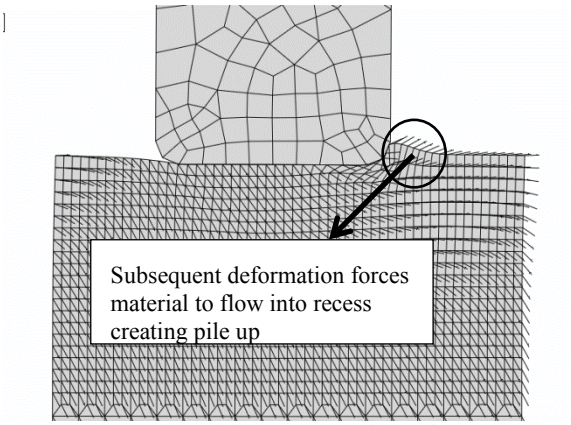

Fig. 4 Material flow in mesoscale simulation

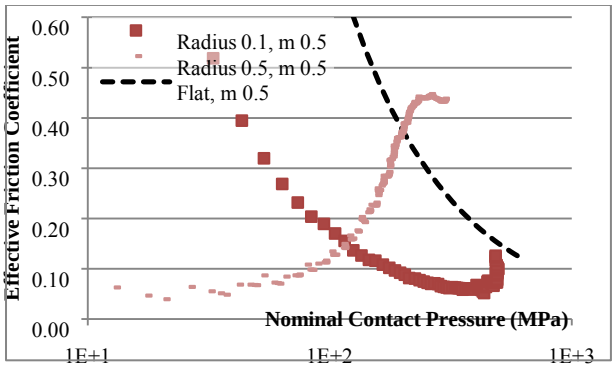

Fig. 5 Constant friction

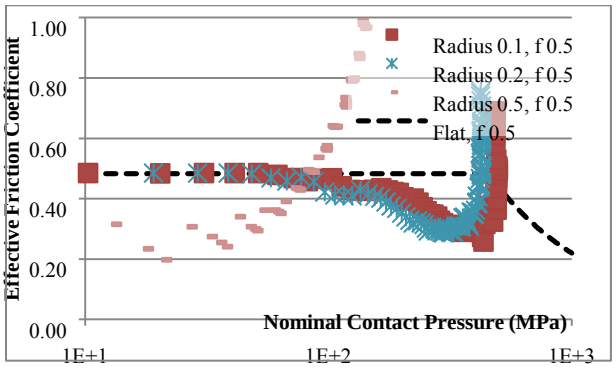

Fig. 6 General friction

The simulation findings can explain how surface textures reduce friction on tribological experiments. At low p_{app}, the surface textures produced smaller load bearing area which in turn limits τ.

In tribological experiments (e.g. tribometer) involving surface textures, the mating bodies do not experience severe plastic deformation to produce plowing by the surface textures because of the relatively low p_{app}, hence the reduced friction when surface textures are introduced.

The influence of mesh refinement was also examined (Fig. 7). All simulations were originally performed using Ratio 20 (Table 3) to provide reasonable number of elements to reproduce the corner radius. Simulation using different element size relative to the texture size (Table 3) was performed using the general friction model with $f = 0.5$ and texture with corner radius of 0.1. For the range of element size simulated, the friction readout was found to be independent of the element size (Fig. 7).

The simulation also disregards the side effects resulted by the imperfection of the surface texturing process. It is noted from past studies [21] that during surface texturing. The method of material removal in order to produce the recess may create material deposit on the perimeter of the recess which affects the performance of the textured surface.

VI. MACROSCALE SIMULATION RESULTS

Macroscale simulation using Deform 2D was performed under axisymmetric geometry to illustrate how surface textures perform in a typical metal forming situation. Forward extrusion geometry with diameter reduction from 6 mm to 4 mm and stroke of 5 mm (Fig. 8) was arbitrarily selected to evaluate the presence of surface textures in bulk metal forming process.

Mechanical property in Fig. 2 was used in the simulation. Two surface profiles (flat and textured with corner radius 0.1) were simulated using general friction factor (f) of 0.5. The friction factor was introduced based on Fig. 6 as pressure-dependent friction stress with extrapolation for nominal contact pressure higher than 500 MPa.

The process load was recorded for the two cases as presented in Fig. 9. Process load in bulk metal forming processes is used to both deform the workpiece material and overcome friction. Therefore, process load was used as indication of reduction of friction in the Deform simulation. The textured surface of radius 0.1 although useful for nominal contact pressure below 500 MPa, does not produce the desirably lower process extrusion load as the average contact pressure during extrusion of the simulated material is much higher than 500 MPa.

However, it is noted that because of the added behavior of macroscopic plowing by surface textures, the distribution of contact pressure in the extrusion process when surface textures are introduced will be different from that using smooth surfaces because of the metal flow into the recess.

TABLE 3 Mesh sensitivity setup

Model Name	El. Size (Tool, Master)	El. Size (Workpiece, Slave)
Ratio 20	0.050	0.036
Ratio 5	0.200*	0.036
Ratio 2	0.500*	0.036
* Corner radiuses were enforced to have at least 2 elements per 90 degrees		

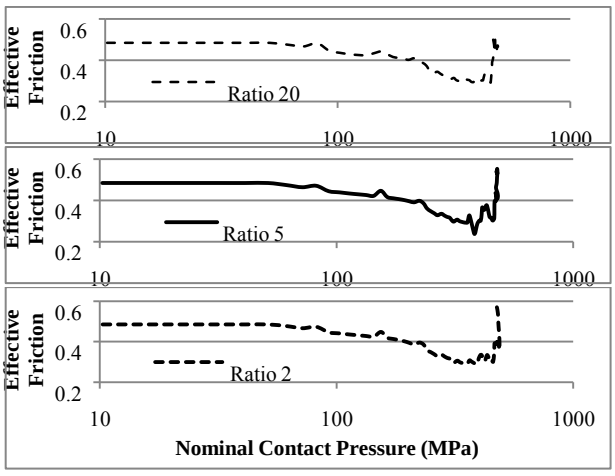

Fig. 7 Influence of mesh size to simulation results

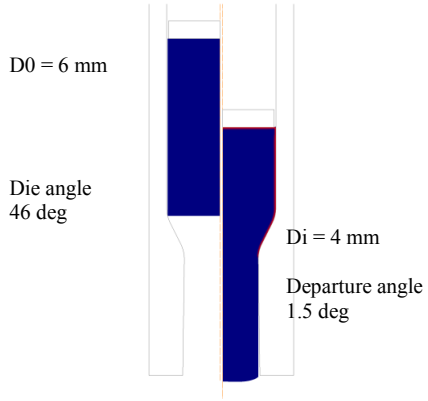

Fig. 8 Forward extrusion simulation setup

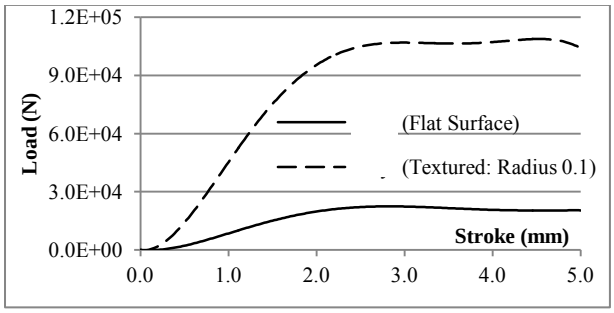

Fig. 9 Process load from extrusion simulations

An application of textured surface for metal forming application was presented in [5]. It was concluded that there is an optimum texture parameter to produce lowest friction in strip drawing test which was designed as friction test for sheet metal forming applications. However, the experimental setup used in [5] only applied 0.11 MPa of contact pressure and the machined grooves were aligned parallel to the sliding direction. Hence the results could not be directly compared with current study.

VII. CONCLUSION

Friction-reducing behavior of textured surfaces was investigated using finite element simulations involving three friction models: Coulomb friction, constant friction, and general friction model. With elastic-plastic material being considered, there are competing behaviors between friction reduction from the reduction of load bearing area (for constant and general friction model) and workpiece plowing from the plastic deformation.

Multi scale simulation approach was presented to exhibit the transfer of friction definition from friction models, to the effective friction definition when surface textures are present. Current simulation results suggest that the introduction of surface textures in bulk metal forming setup is not beneficial. However, the added behavior of macroscopic plowing by the surface textures at high nominal contact pressure may change the distribution of die pressure in bulk metal forming and direct transfer of effective friction in meso-macroscale simulation may not be accurate in determining the real behavior when surface textures are present.

ACKNOWLEDGMENT

This work was funded by NTU Start-up Grant M58050011 and was also supported by the Singapore Institute of Manufacturing Technology (SIMTech) through Forming Technology Group.

REFERENCES

[1] M. Geiger, M. Kleiner, R. Eckstein, N. Tiesler, U. Engel, "Microforming," *CIRP Annals - Manufacturing Technology,* 50 (2001) 445-462.

[2] F. Vollertsen, D. Biermann, H. N. Hansen, I. S. Jawahir, K. Kuzman, "Size effects in manufacturing of metallic components," *CIRP Annals - Manufacturing Technology,* 58 (2009) 566-587.

[3] S. Schreck, K. H. Zum Gahr, "Laser-assisted structuring of ceramic and steel surfaces for improving tribological properties," *Applied surface science,* 247 (2005) 616-622.

[4] A. Borghi, E. Gualtieri, D. Marchetto, L. Moretti, S. Valeri, "Tribological effects of surface texturing on nitriding steel for high-performance engine applications," *Wear,* 265 (2008) 1046-1051.

[5] E. Brinksmeier, O. Riemer, S. Twardy, "Tribological behavior of micro structured surfaces for micro forming tools," *International Journal of Machine Tools and Manufacture,* 50 (2010) 425-430.

[6] Y. Uehara, M. Wakuda, Y. Yamauchi, S. Kanzaki, S. Sakaguchi, "Tribological properties of dimpled silicon nitride under oil lubrication," *Journal of the European Ceramic Society,* 24 (2004) 369-373.

[7] M. Wakuda, Y. Yamauchi, S. Kanzaki, Y. Yasuda, "Effect of surface texturing on friction reduction between ceramic and steel materials under lubricated sliding contact," *Wear,* 254 (2003) 356-363.

[8] M. Suh, Y. Chae, S. Kim, T. Hinoki, A. Kohyama, "Effect of geometrical parameters in micro-grooved crosshatch pattern under lubricated sliding friction," *Tribology International,* 43 (2010) 1508-1517.

[9] N. P. Suh, M. Mosleh, P. S. Howard, "Control of friction," *Wear,* 175 (1994) 151-158.

[10] P. Suh, "The delamination theory of wear," *Wear,* 25 (1973) 111-124.

[11] X. Wang, K. Kato, K. Adachi, K. Aizawa, "The effect of laser texturing of sic surface on the critical load for the transition of water lubrication mode from hydrodynamic to mixed," *Tribology International,* 34 (2001) 703-711.

[12] F. P. Bowden, D. Tabor, *The friction and lubrication of solids* vol. 1: Oxford University Press, USA, 2001.

[13] B. Avitzur, *Metal forming: Processes and analysis*: McGraw-Hill, 1968.

[14] S. Petersen, P. Martins, N. Bay, "Friction in bulk metal forming: A general friction model vs. The law of constant friction," *Journal of Materials Processing Technology,* 66 (1997) 186-194.

[15] T. Wanheim, N. Bay, A. S. Peterson, "A theoretically determined model for friction in metal forming processes," *Wear,* 28 (1974) 251-258.

[16] X. Tan, "Comparisons of friction models in bulk metal forming," *Tribology International,* 35 (2002) 385-393.

[17] N. Bay, "Friction stress and normal stress in bulk metal-forming processes," *Journal of Mechanical Working Technology,* 14 (1987) 203-223.

[18] X. Tan, P. Martins, N. Bay, W. Zhang, "Friction studies at different normal pressures with alternative ring-compression tests," *Journal of Materials Processing Technology,* 80 (1998) 292-297.

[19] S. Stupkiewicz, *Micromechanics of contact and interphase layers*: Springer, 2007.

[20] G. E. Dieter, H. A. Kuhn, S. L. Semiatin, *Handbook of workability and process design*: ASM International, 2003.

[21] A. Kovalchenko, O. Ajayi, A. Erdemir, G. Fenske, I. Etsion, "The effect of laser surface texturing on transitions in lubrication regimes during unidirectional sliding contact," *Tribology International,* 38 (2005) 219-225.